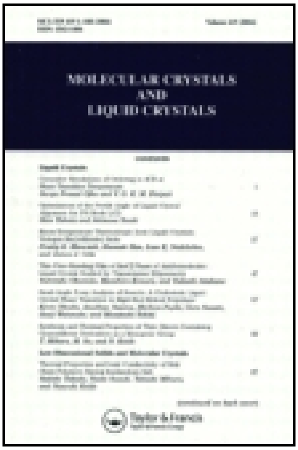

Molecular Crystals and Liquid Crystals Science and Technology. Section A. Molecular Crystals and Liquid Crystals

Publication details, including instructions for authors and subscription information:
http://www.tandfonline.com/loi/gmcl19

Alignment of Liquid Crystal by Patterned Isotropic Surfaces

Baek-Woon Lee [a] & Dongsik Sagong [a]

[a] Samsung Electronics Corp., AMLCD Div., Basic Research Team Gyeonggi-do, Yongin-si, Giheung-eup, Nongseo-ri, San 24, S. KOREA

Version of record first published: 24 Sep 2006

To cite this article: Baek-Woon Lee & Dongsik Sagong (2001): Alignment of Liquid Crystal by Patterned Isotropic Surfaces, Molecular Crystals and Liquid Crystals Science and Technology. Section A. Molecular Crystals and Liquid Crystals, 364:1, 519-528

To link to this article: http://dx.doi.org/10.1080/10587250108025022

Mol. Cryst. and Liq. Cryst., 2001, Vol. 364, pp. 519-528
Reprints available directly from the publisher
Photocopying permitted by license only

Published by license under the
Gordon and Breach Science Publishers imprint,
a member of the Taylor & Francis Group,
Printed in the USA

Alignment of Liquid Crystal by Patterned Isotropic Surfaces

BAEK-WOON LEE and DONGSIK SAGONG

Samsung Electronics Corp., AMLCD Div., Basic Research Team Gyeonggi-do,
Yongin-si, Giheung-eup, Nongseo-ri, San 24, S. KOREA

Alignment of Liquid Crystals (LCs) has been mostly achieved by microscopically anisotropic surfaces. It is widely believed that anisotropic van der Waals interaction is responsible for the alignment of LCs. We report that isotropic surfaces can align LCs as well when patterned topologically, chemically, and electrically. Stripe-patterned surfaces were produced by photolithography, having periodicity of several microns. The surfaces have either undulation (high and low, topological), alternating polar easy axes (planar and homeotropic, chemical), or alternating conductivity (conducting and non-conducting, electrical). LCs were aligned perpendicularly to the electrical pattern, in contrast to the topological and chemical patterns to which LCs were aligned tangentially. Topologically patterned isotropic surfaces align LCs by the well-known Berreman mechanism. In this report, it is analytically shown that elastic anisotropy and flexoelectricity are responsible for the azimuthal anchoring of LCs on the chemically and electrically patterned surfaces, respectively.

Keywords: alignment; elastic anisotropy; flexoelectricity; patterned surface; isotropic; self-assembled monolayer

INTRODUCTION

Liquid Crystals (LCs) have been popularly utilized in electro-optic devices. Director configuration, thus retardation of light passing through LC, with no electric field applied is elastically determined from the alignment at the bounding surfaces. Electric field distorts the initial configuration and consequently the retardation, giving contrast.

The two most popular methods to align LCs are mechanical rubbing [1] and photo-alignment [2]. These two methods generate chemically anisotropic surface and/or undulation of the surface. LC molecules orient themselves in such a way as to minimize the surface free energy. On grooved surfaces, LC molecules align by the well-known Berreman mechanism [3]. In the presence of chemically anisotropic surfaces, it is widely believed that anisotropic van der Waals interaction is responsible for aligning LC molecules [4], although this theory has been in dispute recently [5]. In addition to these two (possibly only one) alignment mechanisms, we show in the report that there are two others: elastic anisotropy and flexoelectricity.

Three types of patterned isotropic surfaces were prepared, which all aligned nematic LC molecules. One surface had alternating heights (topological pattern), another had alternating polar easy axes (chemical pattern), and the other had stripes of Indium Tin Oxide (ITO) electrodes (electrical pattern). Since all surfaces are isotropic, the effect of anisotropic van der Waals interaction is excluded, if any. Furthermore, the chemically patterned surfaces were prepared with UV-patterned Self-Assembled Monolayer (SAM, 20 Å thick) and the thickness of the ITO electrodes for the electrically patterned surface was only 400 Å. Therefore, the Berreman mechanism does not apply to these two surfaces. We show analytically that the two new alignment mechanisms result from elastic anisotropy and flexoelectricity, respectively.

EXPERIMENT

The three types of patterned isotropic surfaces were fabricated with photolithographic masks having a pattern of stripes of several microns in width. The structures of the surfaces are shown in FIGURE 1. For topologically and electrically patterned surfaces (T-surface and E-surface, respectively), 400 Å of ITO was deposited onto glass by sputtering. Novolac PhotoResist (PR) was spin-coated on the ITO glass, subsequently exposed to UV through a photo-mask, and developed. The resulting surface (T-surface) had 2.0 μm high periodic mounds. The profile of the PR was about 45° . The T-surface was further etched with hydrochloric and acetic acid and the PR was stripped off to produce E-surface. ITO glass with a homeotropic polyimide alignment layer of 700 Å printed was used as the opposing substrate for T- and E-surfaces. The cell gap was 4.5 μm.

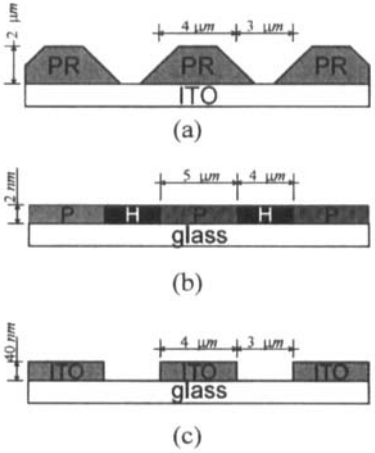

FIGURE 1. The structures of (a) topologically, (b) chemically (Planar and Homeotropic), and (c) electrically patterned surfaces.

For chemically patterned surface (C-surface), glass substrates were dipped in a bath of toluene solution of 2% OctadecylTriEthoxy-Silane (OTE) [6]. Self-Assembled Monolayer (SAM) was formed on the surface and it induced homeotropic anchoring. Upon UV exposure of about 5 KJ/cm^2, the SAM became hydrophilic, inducing planar alignment with no preferred azimuthal easy axis. Atomic Force Microscopy (AFM) revealed that the UV-exposed region was about 10 Å lower than the unexposed [7]. It is quite possible that the height difference resulted from the depression by the tip of the AFM, rather than it was real topography. In any case, the height difference is negligible in terms of the Berreman mechanism. Unexposed SAM on glass was used as the opposing substrate.

The assembled cells were filled with LC in the isotropic phase. The LC mixture had a wide temperature range of nematic phase (-40 ~ 87.0 °C), $\Delta n = 0.088$, $\Delta\varepsilon = 7.4$, and no chiral dopant. The cells were investigated with a polarizing microscope and an aid of a compensator.

RESULTS AND DISCUSSION

Three cells consisting of the three types of surfaces and the opposing substrates with homeotropic alignment layer are shown in FIGURE 2. The left areas of (a) and (c) were not patterned, and as expected from isotropic surfaces, the cells exhibited Schlieren texture: LC molecules point in arbitrary azimuthal direction. However, the nematic LC director was all aligned parallel or perpendicular to the stripes in the patterned areas. With an aid of a compensator, we could determine the azimuthal direction of the director unambiguously. The nematic director was turned out to be perpendicular to the stripes on E-surface in contrast to T- and C-surfaces on which the director was parallel to the stripes.

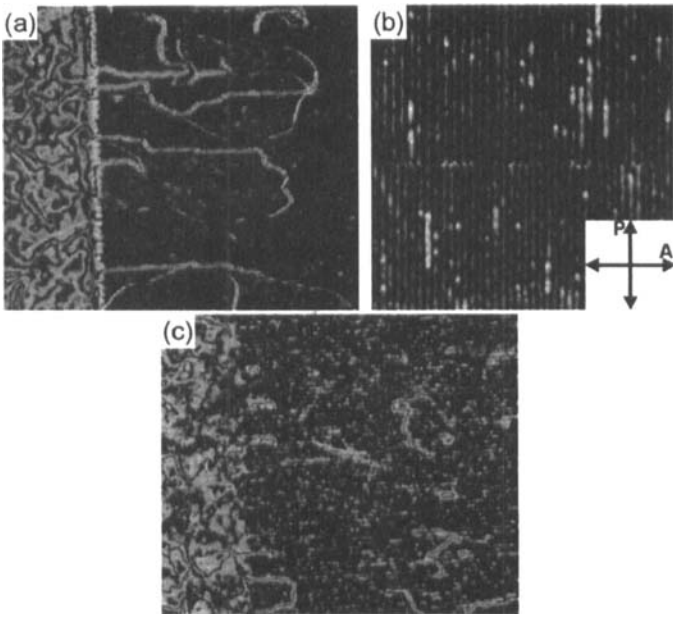

FIGURE 2. Alignment by patterned isotropic surfaces. (a) topologically patterned. (b) chemically patterned. (c) electrically patterned. The disclination lines separate domains of two tilt directions.

The LC molecules align on T-surface (not surprisingly) by the Berreman mechanism [FIGURE 3(a)]. Using the one-constant approximation and assuming $A/\lambda << 1$, for a surface whose profile is given as the following,

$$\xi(x) = A\sin\left(\frac{2\pi}{\lambda}x\right) \quad \text{................................(Eq. 1)}$$

the azimuthal anchoring energy is given by [3],

$$W_a(\phi) = W_a \sin^2\left(\phi - \frac{\pi}{2}\right) \quad \text{.............................(Eq. 2)}$$

where $W_a = 2\pi^3 A^2 K/\lambda^3$ (Eq. 3).

Since C- and E-surfaces do not have significant height variation, the Berreman mechanism does not apply to these surfaces. For a nematic director $\mathbf{n} = \mathbf{n}(\theta, \phi)^*$, the Frank elastic free energy is divided into two parts:

$$F = F_1(\theta) + F_2(\theta,\phi)$$

$$= \frac{1}{2}\left\{K_b(\nabla\theta)^2 - (K_b - K_t)\sin^2\phi\left(\frac{\partial\theta}{\partial x}\right)^2 \right. \quad \text{............(Eq. 4a)}$$

$$\left. -(K_b - K_s)\left(\cos\phi\cos\theta\frac{\partial\theta}{\partial x} - \sin\theta\frac{\partial\theta}{\partial z}\right)^2\right\}$$

$$F_2(\theta,\phi) = (K_b - K_s)\cos\phi\sin\theta\cos\theta\frac{\partial\theta}{\partial x}\frac{\partial\theta}{\partial z}$$

$$+\frac{1}{2}\{(K_s - K_t) + (K_b - K_s)\sin^2\theta\}\sin^2\left(\phi - \frac{\pi}{2}\right)\left(\frac{\partial\theta}{\partial x}\right)^2 \quad \text{.(Eq. 4b)}$$

The first term in Eq. 4b yields zero when integrated over a period λ, assuming $\phi = const.$ The second term has the same form as Eq. 2, with

$$W_a = \frac{1}{2\lambda}\int_0^\infty\int_0^\lambda \{(K_s - K_t) + (K_b - K_s)\sin^2\theta\}\left(\frac{\partial\theta}{\partial x}\right)^2 dxdz \quad \text{..(Eq. 5)}$$

---

[*] Throughout the paper, the z-axis is taken to be normal to the substrates and the y-axis is in the direction of the stripes. θ is the polar angle, measured from the z-axis and ϕ is the azimuth, from the x-axis.

This can be quite significant when $\partial\theta/\partial x$ is large, as is the case for the C-surface on which θ changes $\pi/2$ over $\lambda/2$. Comparison with Eq. 3 shows that the elastic anisotropy substitutes for the one-constant K, and $\Delta\theta$, the difference of the polar easy axes of the two adjacent surfaces acts as the height variation amplitude $2A$. The polar angle $\theta(x, z)$ can be analytically calculated [8] with the one-constant approximation [9] and the integral of Eq. 5 can be carried out. The azimuthal anchoring energy assumes the form of $\sim K/\lambda \sim 10^{-11}/10^{-5} = 10^{-6}$ J/m^2, which is quite large and comparable to that of a rubbed surface.

The C-surface is comprised of stripes of unexposed SAM (homeotropic alignment inducing, H-stripe) and UV-exposed SAM (planar alignment inducing, P-stripe) [FIGURE 1(b)]. Going from homeotropic to planar, the LC director may adopt splay-bend deformation ($\phi = 0°$), or twist ($\phi = 90°$) [FIGURE 3(b)]. Since, for typical LCs, splay-bend costs more energy than twist (elastic anisotropy), the nematic director adopts twist deformation: LC molecules align tangentially to the stripes [10].

For the E-surface, the second term in Eq. 4b becomes negligible since both ITO and glass induce planar anchoring. The particular alignment geometry of the LC cell induces splay-bend deformation going planar at the bottom to homeotropic at the top. Flexoelectric polarization associated with the deformation is developed in the deformation plane [FIGURE 3(c) left]. Therefore, the free energy must include an additional term, $-\mathbf{P}\bullet\mathbf{E}$. Since the azimuthal direction ϕ of the nematic director is assumed to be constant throughout the whole cell, the electric field from "other" flexoelectric polarization does not contribute to the azimuthal anchoring energy. Only the electric field from the charges on the surface (mostly on the electrodes) induced by the polarization itself may affect the azimuthal anchoring. By symmetry, the E-field can exist only in the xz-plane. The free energy can be lowered if the flexoelectric polarization is also in the xz-plane: ϕ

= 0°, or the projection of the nematic director onto the substrates is *perpendicular* to the stripes.

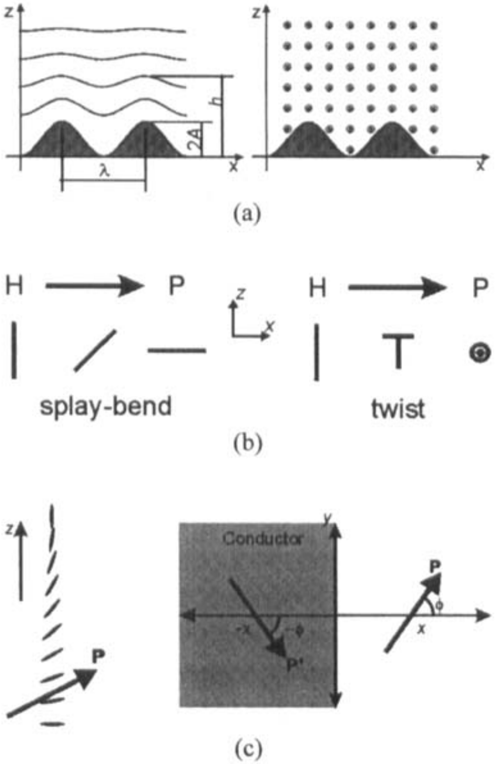

FIGURE 3. Alignment mechanisms for the patterned isotropic surfaces. (a) T-surface: the Berreman mechanism. (b) C-surface: elastic anisotropy. Going **Homeotropic** to **Planar**, splay-bend costs more elastic energy than twist. (c) E-surface: flexoelectricity. The interaction energy between a flexoelectric polarization and the image is minimized when the polarization is parallel to the x-axis.

Exact calculation of the anchoring energy is complicated. The flexoelectric polarization depends on the director configuration and the director itself is affected by the induced electric field from "other" flexoelectric polarization as well as from the charges on the surfaces. However, we can focus on a periodic segment of the E-surface ($z = 0$ plane) and get a glimpse of what form the anchoring energy may assume. Imagine a 2D-system where a polarization **p** exists at $x > 0$, forming an angle ϕ with the x-axis and a conductor fills the other half-plane $x < 0$ [FIGURE 3(c) right]. An image polarization **p**' exists at $-x$, forming an angle $-\phi$ with the x-axis. The interaction energy is given by

$$\begin{aligned} W &= \frac{\mathbf{p}\bullet\mathbf{p}'-3(\mathbf{x}_0\bullet\mathbf{p})(\mathbf{x}_0\bullet\mathbf{p}')}{|\mathbf{x}-\mathbf{x}'|^3} = \frac{p^2\cos 2\phi - 3p^2\cos^2\phi}{8x^3} \\ &= -\frac{p^2}{8x^3}(1+\cos^2\phi) \Rightarrow \frac{p^2}{8x^3}\sin^2\phi \end{aligned} \qquad \text{.....(Eq. 6)}$$

It has the same quadratic sinusoidal dependence as the T- and C-surfaces.

CONCLUSION

We prepared two such kinds of surfaces that the two most common alignment mechanisms, the Berreman mechanism and anisotropic van der Waals interaction, do not apply. Chemically patterned surface aligned LC molecules tangentially to the pattern and electrically patterned surface aligned LC perpendicularly. Two novel mechanisms for LC alignment are suggested: elastic anisotropy and flexoelectricity.

References

[1] J. Cognard, *Mol. Cryst. Liq. Cryst., Suppl. 1*, **78**, 1 (1982).

[2] W. M. Gibbons, P. J. Shannon, S. T. Sun, and B. J. Swetlin, *Nature* **351**, 49 (1991); P. J. Shannon, W. M. Gibbons, and S. T. Sun, *Nature* **368**, 532 (1994); W. M. Gibbons and S. T. Sun, *Appl. Phys. Lett.* **65**, 2542 (1994); W. M. Gibbons, T. Kosa, P. Palffy-Muhoray, P. J. Shannon, and S. T. Sun, *Nature* **377**, 43 (1995); T. Ikeda and O. Tsutsumi, *Sci-*

ence **268**, 1873 (1995); J. Chen, D. L. Johnson, P. J. Bos, S. Sprunt, J. Lando, and J. A. Mann, Jr., *Appl. Phys. Lett.* **68**, 885 (1996).

[3] D. W. Berreman, *Phys. Rev. Lett.* **28**, 1983 (1972); S. Faetti, *Phys. Rev. Lett.* **36**, 408 (1987); S. Faetti, M. Nobili, and A. Schirone, *Liq. Cryst.* **10**, 95 (1991).

[4] P. G. de Gennes, *C. R. Acad, Sci. B* **271**, 469 (1970); E. R. Smith and B. W. Ninham, *Physica* **66**, 111 (1973); K. Okano, N. Matsuura, and S. Kobayashi, *Jpn. J. Appl. Phys.* **21**, L109 (1982).

[5] J.-H. Kim, Y. Shi, B. Acharya, and S. Kumar, *to be published.*

[6] J. F. Mooney, A. J. Hunt, J. R. McIntosh, C. A. Liberko, D. M. Walba, and C. T. Rogers, *Proc. Natl. Acad. Sci. USA* **93**, 12287 (1996).

[7] B. -W. Lee and N. A. Clark, *Langmuir* **14**, 5495 (1998).

[8] B. -W. Lee and N. A. Clark, *submitted to Liq. Cryst.*; B.-W. Lee, Ph. D dissertation, University of Colorado at Boulder (1998).

[9] The inclusion of elastic anisotropy modifies the director configuration. However, for a typical nematic LC whose magnitudes of the elastic constants are in the following order $K_b > K_s > K_t$, the director configuration is very similar to that of the isotropic case [8].

[10] B.-W. Lee and N. A. Clark, *submitted to Science.*